Proc. Natl. Acad. Sci. USA
Vol. 96, pp. 3269–3274, March 1999
Neurobiology

Ca^{2+}/calmodulin-kinase II enhances channel conductance of α-amino-3-hydroxy-5-methyl-4-isoxazolepropionate type glutamate receptors

VICTOR DERKACH, ANDRES BARRIA, AND THOMAS R. SODERLING*

Vollum Institute, Oregon Health Sciences University, Portland, OR 97201

Edited by Michael V. L. Bennett, Albert Einstein College of Medicine, Bronx, NY, and approved December 29, 1998 (received for review September 11, 1998)

ABSTRACT **The ability of central glutamatergic synapses to change their strength in response to the intensity of synaptic input, which occurs, for example, in long-term potentiation (LTP), is thought to provide a cellular basis for memory formation and learning. LTP in the CA1 field of the hippocampus requires activation of Ca^{2+}/calmodulin-kinase II (CaM-KII), which phosphorylates Ser-831 in the GluR1 subunit of the α-amino-3-hydroxy-5-methyl-4-isoxazolepropionate glutamate receptor (AMPA-R), and this activation/phosphorylation is thought to be a postsynaptic mechanism in LTP. In this study, we have identified a molecular mechanism by which CaM-KII potentiates AMPA-Rs. Coexpression in HEK-293 cells of activated CaM-KII with GluR1 did not affect the glutamate affinity of the receptor, the kinetics of desensitization and recovery, channel rectification, open probability, or gating. Single-channel recordings identified multiple conductance states for GluR1, and coexpression with CaM-KII or a mutation of Ser-831 to Asp increased the contribution of the higher conductance states. These results indicate that CaM-KII can mediate plasticity at glutamatergic synapses by increasing single-channel conductance of existing functional AMPA-Rs or by recruiting new high-conductance-state AMPA-Rs.**

Long-term potentiation (LTP) is a prolonged enhancement in synaptic efficacy thought to underlie certain forms of learning and memory, and recent studies have begun to unravel mechanisms that may be involved in this phenomenon (1, 2). It has been shown that LTP in the CA1 field of the hippocampus requires elevation of calcium in the postsynaptic spine and is accompanied by activation of Ca^{2+}/calmodulin-kinase II (CaM-KII; refs. 3–5), which phosphorylates α-amino-3-hydroxyl-5-methyl-4-isoxazole-propionate glutamate receptors (AMPA-Rs; ref. 6). CaM-KII has unusual biochemical properties that make it a unique transducer of postsynaptic Ca^{2+} signaling (7–9). AMPA-Rs, which are comprised of subunits GluR1–GluR4, are primarily responsible for the enhanced synaptic current during expression of LTP (1, 2). AMPA-R current in cultured hippocampal neurons (10) or synaptic current in CA1 pyramidal neurons of hippocampal slices (11, 12) can be enhanced by infusion or expression of activated CaM-KII. This CaM-KII-mediated potentiation of synaptic current occludes the ability to induce LTP subsequently, suggesting that they share common mechanisms. Phosphorylation by CaM-KII or protein kinase C of Ser-831 in GluR1, a site unique to the intracellular COOH terminus of the GluR1 subunit, potentiates receptor current (13, 14). In this paper, we have investigated the molecular mechanism by which CaM-KII phosphorylation of Ser-831 in GluR1 potentiates its current, and our data show that CaM-KII significantly increases the occurrence of high-conductance states in GluR1 channel activity. Because induction of LTP often results in an increase in single-channel conductance of postsynaptic AMPA-Rs (15), our results indicate one molecular mechanism by which CaM-KII mediates synaptic plasticity.

EXPERIMENTAL METHODS

Experiments were performed on HEK-293 cells expressing GluR1 receptor subunit either alone or with a constitutively active mutant of CaM-KII (His-282 to Arg) as described (6, 13). *In vitro* mutagenesis of Ser-831 to Asp and Glu in GluR1 was performed by using the Quick change site-directed mutagenesis kit from Stratagene and was checked by sequencing (13). Patch pipettes were filled with (in mM) 160 CsCl, 2 $MgCl_2$, 4 Na_2ATP, 1 EGTA, and 10 Hepes. Extracellular solution contained (in mM) 165 NaCl, 2.5 KCl, 1 $MgCl_2$, 2 $CaCl_2$, and 5 Hepes. Constitutively active and heat-inactivated (HI) CaM-KII at 0.4 μM was added to the patch pipette where indicated. Series resistance was below 11 MΩ and 60–80% compensated. Glutamate was applied to the lifted cells or outside-out patches by a piezo-driven application system. The rate of solution exchange was 1–3 ms ($n = 5$) and 0.2–0.5 ms ($n = 6$) for whole-cell and outside-out patches, respectively, determined as the time for a 10–90% change in the current amplitude during application of 30% diluted external solution to the cell or patch. Macroscopic currents were collected at a 0- to 2-kHz bandwidth and digitized at 10 kHz. Kinetic parameters of glutamate-evoked currents were obtained by simultaneously fitting their rising and decaying phases by the sum of two exponentials (PCLAMP6 software).

Nonstationary fluctuation analyses (16) were performed for the currents evoked by 70- to 100-ms applications of 10 mM glutamate at time intervals of 4 s. From 36 to 93 currents were collected for each analysis, with allowed run-down below 10%. Single-channel currents were recorded in the cell-attached mode at 0- to 2-kHz bandwidth and were digitized at 20 kHz. GluR1 channel activity was evoked by the inclusion of 10 μM AMPA in the patch pipette and was recorded at pipette holding potentials of 70 mV or 80 mV. Membrane potential (−35 mV to −51 mV) was measured immediately after cell-attached observations within the first 3 s of the whole-cell configuration. GluR1-channel activity was identified as (*i*) currents that were present uniquely in the patches with AMPA as the agonist from only those cells having whole-cell current on application of 10 mM glutamate (18 patches from 18 cells) and never observed in cells without the glutamate-evoked

The publication costs of this article were defrayed in part by page charge payment. This article must therefore be hereby marked "*advertisement*" in accordance with 18 U.S.C. §1734 solely to indicate this fact.

PNAS is available online at www.pnas.org.

This paper was submitted directly (Track II) to the *Proceedings* office.
Abbreviations: AMPA-R, α-amino-3-hydroxy-5-methyl-4-isoxazolepropionate glutamate receptor; CaM-KII, Ca^{2+}/calmodulin-kinase II; HI, heat-inactivated; LTP, long-term potentiation.
*To whom reprint requests should be addressed. e-mail: soderlit@ohsu.edu.

currents (137 patches, 1 per cell); (*ii*) currents that were never observed in the presence of AMPA and 20 μM 6-cyano-7-nitroquinoxaline-2,3-dione in the patch pipette from cells that had glutamate-evoked currents (58 patches, 1 per cell); and (*iii*) currents that had a strong inward rectification (no currents recorded at potentials of 60–80 mV). For analyses, channel activity was digitally filtered further at 1–1.5 kHz. Such filtering provided optimal detection of elementary currents (17). Particularly at driving forces varied from 115 mV to 141 mV and σ_{noise} of the background noise from 0.064 pA to 0.096 pA, this filtering provided a signal-to-noise ratio of at least 7 for the minimal conductance level observed of 5 pS. The threshold for detection of elementary currents was set at $5\sigma_{noise}$, which generated the rate of false events of <3% of all detected events. σ_{noise} of background noise was controlled periodically during analyses to ensure the stability of detection conditions. The estimated amplitude of the event was controlled by the operator on superimposition of acquired and simulated events before the event was accepted for further analysis. The duration of events was determined at half the current amplitude, and the resolution limit for each event was set at 0.2 ms or 0.3 ms for 1.5-kHz and 1-kHz filtrations, respectively. Weighted single-channel conductance was calculated from each conductance distribution as $\gamma_{mean} = \Sigma\alpha_n\gamma_n$, where γ_n and α_n are a conductance and its contribution to the distribution, respectively, and n is the number of conductance components. All recordings were performed at room temperature (21–22°C). Statistical significance was evaluated by Student's two-tailed t test ($P < 0.05$).

RESULTS

Several receptor parameters could be affected by phosphorylation and contribute to the potentiating effect of CaM-KII on AMPA-R current. We examined those parameters in HEK-293 cells expressing GluR1 alone or coexpressed with activated CaM-KII, which greatly enhances phosphorylation of GluR1 at Ser-831 (13, 14). Expressed GluR1 in HEK-293 cells seems to be a valid model, because potentiation of its current by CaM-KII (6, 13) closely mimics potentiation of AMPA-R/synaptic current in cultured hippocampal neurons or hippocampal slices by infused or expressed CaM-KII (10–12). Fig. 1*A* shows that dose–response curves for glutamate in these two situations were remarkably similar with EC_{50} and Hill coefficients of about 0.7 mM and 1.1, respectively, either with or without CaM-KII coexpression (Table 1). This result indicated no significant effect of CaM-KII on GluR1 affinity for glutamate and was not a likely mechanism for GluR1 current potentiation in our previous experiments (6, 13) as we used a saturating concentration of glutamate (10 mM).

However, the number of functional receptors (N), channel conductance (γ), channel open probability (P_o), and the electrochemical potential through the channel ($V - V_{rev}$, where V is the membrane potential and V_{rev} is the reversal potential for the current) could theoretically contribute to the CaM-KII potentiation, because they determine the AMPA-R peak current (I) through their product: $I = \gamma NP_o(V - V_{rev})$. Fig. 1 *B* and *C* shows *I–V* curves for GluR1 in whole-cell and outside-out patch recording configurations. There were no significant shifts in V_{rev} in either configuration with or without coexpressed CaM-KII (Table 1). Under whole-cell conditions, *I–V* curves exhibited a strong inward rectification (Fig. 1*B Lower*) that was reduced dramatically on excision of patches (Fig. 1*C Lower*), consistent with a voltage-dependent inhibition of AMPA-Rs by endogenous polyamines (18). Release from polyamine block on CaM-KII phosphorylation could be a mechanism for the potentiation of GluR1 currents. Because the rectification index (18) was not affected by coexpression with CaM-KII (Fig. 1*D*; Table 1), an effect of CaM-KII on polyamine block was unlikely. Ser-831 in GluR1 is the regulatory CaM-KII phosphorylation site (13, 14); therefore, we attempted to mimic the kinase effect by introducing a negative charge through mutation of Ser-831 to glutamate and aspartate (S831E and S831D, respectively). The mutants were functional receptors, and their analyses confirmed the negative result on polyamine block, as both had rectification properties indistinguishable from those of the wild-type GluR1 receptor (Table 1).

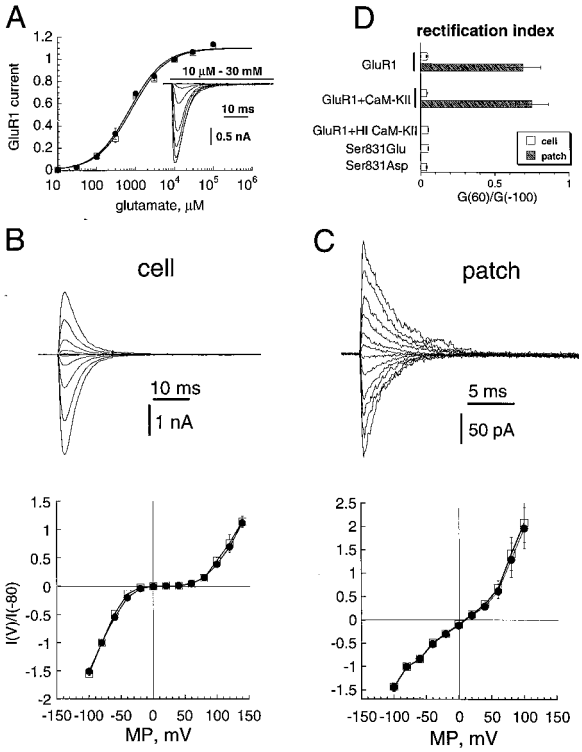

FIG. 1. Effect of CaM-KII on affinity and voltage-dependence of GluR1. (*A*) Dose–response curves for GluR1 with (squares; $n = 4$) and without (circles; $n = 4$) coexpressed CaM-KII. Currents were normalized to those evoked by 10 mM glutamate. (*Insert*) Whole-cell currents elicited at −80 mV by 10 μM to 30 mM glutamate for GluR1 expressed alone. (*B* and *C Upper*) Whole-cell (*B*) and outside-out patch (*C*) currents for GluR1 alone elicited by 100-ms pulses of 10 mM glutamate at membrane potentials from −100 mV to 120 mV (20-mV steps). (*B* and *C Lower*) Voltage-dependence of whole-cell (*B*) and outside-out patch (*C*) currents for GluR1 alone (circles) or for GluR1 coexpressed with CaM-KII (squares). (*D*) Rectification index for whole-cell (open bars) and outside-out patch (gray bars) currents for GluR1 expressed alone, for GluR1 coexpressed with CaM-KII, for GluR1 with HI CaM-KII infused in the patch pipette, and for Ser-831-to-Glu and Ser-831-to-Asp mutants.

Desensitization of GluR1, which occurs within milliseconds (19, 20), could attenuate peak current by decreasing P_o. This attenuation was particularly true for whole-cell current, where the rate of agonist delivery was limited by cell geometry. Indeed, the rate of AMPA-R desensitization by glutamate was about 15–30% slower for whole-cell than for outside-out patch recordings (Fig. 2 *A* and *B*), reflecting perhaps an asynchronization in channel activation and thus in desensitization. We, however, did not observe an acceleration of this rate on saturation of the agonist-binding step at glutamate concentrations above 1 mM (Fig. 2*C*), indicating the recording of an intrinsic transition to a desensitized state. We used 10 mM glutamate to assess the rate of desensitization. Desensitization, tested either in whole-cell or in outside-out patches, was not affected detectably by CaM-KII coexpression or by the mutations of Ser-831 (Fig. 2 *A*, *B*, and *D*; Table 1). In addition, no changes were found in the rate of recovery from desensitization (Fig. 2 *E* and *F*; Table 1). Together, these observations

Table 1. Effect of CaM-KII (KII) and mutations of Ser831 (S831) to Glu (E) or Asp (D) on parameters of GluR1 (R1) tested as a population

Receptor	EC_{50}, μM	n_H	V_{rev}, mV	Rectification index $G(60)/G(-100)$	τ_{des}, ms	τ_{rec}, ms	γ,† pS	P_o†
R1 alone								
Cell	750 ± 50	1.1 ± 0.04	8.7 ± 2.2	0.045 ± 0.006	3.1 ± 0.12	98 ± 9	11.5 ± 1.3	0.79 ± 0.05
	(4)	(4)	(13)	(10)	(17)	(7)	(4 + 3)‡	(4 + 3)‡
Patch	—	—	9.2 ± 1.6	0.69 ± 0.12	2.5 ± 0.16	—	—	—
	—	—	(4)	(4)	(11)	—	—	—
R1 + KII								
Cell	690 ± 140	1.1 ± 0.14	7.8 ± 1.2	0.043 ± 0.004	2.9 ± 0.12	112 ± 11	19.9 ± 1.2**	0.72 ± 0.06
	(4)	(4)	(18)	(12)	(23)	(6)	(3 + 2)‡	(3 + 2)‡
Patch	—	—	8.1 ± 2.0	0.75 ± 0.11	2.3 ± 0.12	—	—	—
	—	—	(5)	(5)	(5)	—	—	—
R1 + HI-KII								
Cell	—	—	8.5 ± 1.5	0.052 ± 0.003	3.3 ± 0.16	—	13.2 ± 1.3	0.83 ± 0.06
	—	—	(7)	(7)	(7)	—	(3 + 1)‡	(3 + 1)‡
S831E RI								
Cell	—	—	6.7 ± 2.7	0.051 ± 0.002	3.1 ± 0.22	127 ± 12	18.7 ± 1.3**	0.64 ± 0.05
	—	—	(6)	(6)	(5)	(4)	(3 + 2)‡	(3 + 2)‡
Patch	—	—	—	—	2.3 ± 0.19	—	—	—
	—	—	—	—	(4)	—	—	—
S831D								
Cell	—	—	7.2 ± 1.6	0.041 ± 0.005	2.9 ± 0.14	122 ± 15	27.5 ± 2.9**	0.62 ± 0.07
	—	—	(15)	(15)	(19)	(3)	(4 + 2)‡	(4 + 2)‡
Patch	—	—	—	—	2.6 ± 0.3	—	—	—
	—	—	—	—	(3)	—	—	—

Means ± SEM are shown, followed by the number of measurements (in parentheses). n_H, Hill coefficient; V_{rev}, reversal potential for the current; G, peak conductance at indicated membrane potential; τ_{des}, time constants of the decays; τ_{rec}, time constant; γ, channel conductance; P_o, channel open probability. **, $P < 0.01$.

†Combined statistic of cells and patches for γ and P_o.

‡Number of cells + number of patches.

indicate that CaM-KII did not modulate receptor desensitization or recovery.

Multiple applications of glutamate to the same patches or cells showed in a significant increase in amplitude of current fluctuations on coexpression or infusion of CaM-KII (Fig. 3 *A* and B *Left*). This result suggested either an increase in single-channel conductance or change in channel P_o. We determined these parameters by applying nonstationary variance analysis (16), which confirmed a significant increase in single-channel conductance with perhaps a slight decrease in P_o (Fig. 3 *A* and *B Right*). It was possible in some outside-out patches (3 of 19 tested) to observe single-channel currents on the tails of macroscopic currents where channel P_o was reduced dramatically by desensitization (Fig. 3*C Left*). Direct measurements of single-channel tail currents independently confirmed their estimation through variance analyses (Fig. 3*C Right*). The analyses identified an ≈70% increase in single-channel conductance on coexpression or infusion of activated CaM-KII (Fig. 3*D Left*; Table 1). In contrast, no significant change in P_o was found (Fig. 3*D Right*; Table 1). The effect of CaM-KII on channel conductance was not observed by infusion of HI CaM-KII but was mimicked by the Glu and Asp mutants (Fig. 3*D*; Table 1). These observations confirmed the critical role of Ser-831 as the regulatory CaM-KII phosphorylation site in GluR1.

We could not directly compare the number of functional GluR1 receptors with or without coexpression of CaM-KII, because independent sets of measurements were used. However, the channel conductance after CaM-KII action was 74 ± 6% greater ($n = 6$) than the conductance in untreated cells that closely matched the increase in whole-cell peak current on infusion of CaM-KII (53 ± 17%; $n = 11$; see refs. 6 and 13). Therefore, it was unlikely that a significant change in the number of receptors contributed to the potentiation of GluR1 current in HEK-293 cells. Previously, we have shown that conditions known to stimulate CaM-KII phosphorylation of AMPA-Rs in hippocampal neurons did not show a detectable increase in their surface expression (21).

Because variance analysis provides only a weighted value for channel conductance, its enhancement by CaM-KII can arise from different mechanisms, including the modification of dwell times in existing states, the appearance of new high-conductance states, or the recruitment of new channels with high-conductance states. We attempted to distinguish these molecular mechanisms by directly analyzing single-channel activity. The cell-attached configuration was chosen over excised patches, because we wanted to maintain the cellular environment of the AMPA-Rs and because excised patches exhibited a rapid run-down of channel activity. Single-channel recordings indicated that the GluR1 channel, similar to GluR4 and GluR2/GluR4 (22), can adopt multiple conductance states with values ranging from 9 pS to 28 pS (Fig. 4*A*; Table 2). High-conductance states could arise artifactually from random superimpositions of single-channel openings from different receptors in the patch. However, chances of such superimpositions were below 0.1% of the total number of events in patches (the total P_o of channel activity in individual patches was below 1%). This value was far below the 20% of high-conductance events observed in control experiments, where their contribution was minimal (Table 2; Fig. 4*A Middle*). When GluR1 was expressed alone, the lower conductance states (9 pS and 14 pS) dominated in the total channel activity (Fig. 4*A Middle*). Coexpression of CaM-KII increased the occurrence of the higher conductance states (21 pS and 28 pS; compare Fig. 4*A Middle* with Fig. 4*B Middle*; Table 2). This redistribution of channel states was confirmed by mutation of Ser-831 to Asp where the high-conductance states comprised about 80% of the total activity (Fig. 4*C Middle*; Table 2). The distribution of channel openings was fitted by two exponentials with time constants of about 0.3 ms and 2 ms for GluR1 alone

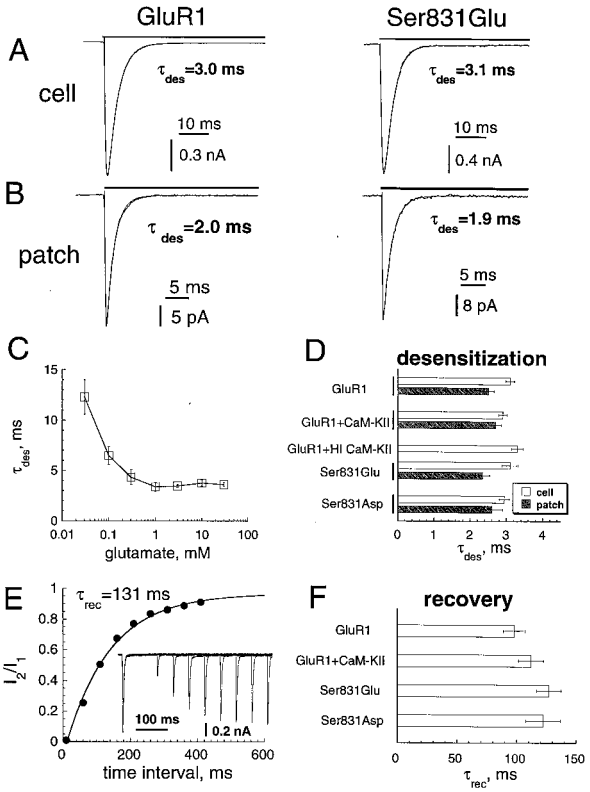

FIG. 2. Effect of CaM-KII on the desensitization of GluR1. (*A* and *B*) Whole-cell (*A*) and outside-out patch (*B*) currents elicited by 10 mM glutamate at −80 mV in cells expressing GluR1 alone (*Left*) or the Ser-831-to-Glu mutant (*Right*). The currents were fitted by the sum of two exponentials for the rise and decay shown by the thin line. (*C*) τ_{des} as a function of glutamate concentration for the whole-cell currents ($n = 4$). (*D*) τ_{des} for whole-cell (open bars) and outside-out (gray bars) currents for GluR1 expressed alone, for GluR1 coexpressed with CaM-KII, for GluR1 with HI CaM-KII in the patch pipette, and for Ser-831-to-Glu and Ser-831-to-Asp mutants. (*E*) Time course of recovery from desensitization measured as the amplitude ratio of the second current to the first in pairs of glutamate applications. Points were fitted by exponential (solid line) with the time constant τ_{rec}. (*Insert*) Currents elicited by paired applications of 10 mM glutamate (20-ms pulses) with time intervals 10–1,000 ms after the end of the first application. (*F*) τ_{rec} for cells with GluR1 alone, for cells with GluR1 and CaM-KII, and for Ser-831-to-Glu and Ser-831-to-Asp mutants.

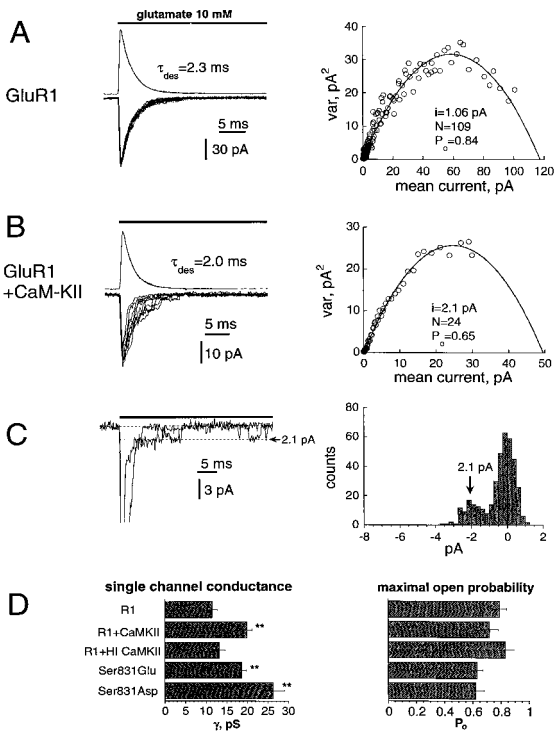

FIG. 3. CaM-KII increased channel conductance. (*A* and *B Left*) Nine currents (downward) elicited by repetitive applications of 10 mM glutamate (70-ms pulses; 4-s time intervals) in outside-out patches when GluR1 was expressed alone (*A*, −90 mV) or with activated CaM-KII in the patch pipette (*B*, −100 mV). The outward currents shown are mean currents for 37 trials (*A*) and 83 trials (*B*). (*A* and *B Right*) The variance of the current fluctuations as a function of the mean currents shown in *A* and *B Left*. Solid lines are fitting curves with the indicated parameters. (*C Left*) Two current traces from the patch shown in *B*, when single-channel currents were resolved on the tails of macroscopic currents. (*C Right*) All-point histogram for traces shown in *C Left*, taken after the decay of macroscopic current. The arrow indicates the value of single-channel current (2.1 pA), determined by the variance analyses. (*D*) Channel conductance (*Left*) and P_o (*Right*), determined by variance analyses when the GluR1 receptor was expressed alone (R1), when the GluR1 receptor was coexpressed with CaM-KII (R1+CamKII), with HI CaM-KII in the patch pipette (R1+HI CaMKII), and of the mutants Ser-831 to Glu and Ser-831 to Asp. **, $P < 0.01$.

(Fig. 4*A Bottom*). This gating of open states was not affected detectably by CaM-KII coexpression or the Ser-831-to-Asp mutation (Fig. 4 *B* and *C Bottom*; Table 2), suggesting that the increased contribution of the higher conductance states to GluR1 phosphorylation was not an effect of better resolution of increased open times. Rather, it was the result of the increased frequency of transitions to the higher conductance states. Weighted single-channel conductance calculated from the conductance distributions was increased from ≈13 pS for GluR1 alone to ≈19 pS on coexpression with CaM-KII and about 22 pS for the Ser-831-to-Asp mutant (Table 2). These changes in weighted single-channel conductances are in a good agreement with our nonstationary fluctuation analysis (Fig. 3; Table 1) and closely match the increase (53%) in macroscopic GluR1 current mediated by CaM-KII (6, 13).

DISCUSSION

Our results show that among several GluR1 receptor parameters capable of potentiating peak current amplitude on phosphorylation by CaM-KII, only channel conductance was increased significantly (Tables 1 and 2). Because the magnitude of the change in channel conductance was sufficiently large to account for the CaM-KII-mediated enhancement of GluR1 peak current, it was unlikely that other parameters, such as a change in the number of functional GluR1 receptors with the same conductance properties, also occurred. If additional functional receptors were recruited, either they could preexist with a P_o of 0, or, if newly inserted, they would have to exhibit high conductance. Modulation of AMPA-R conductance by CaM-KII—and presumably by protein kinase C, because both kinases phosphorylate the same site (13, 14)—is unusual for glutamate-gated channels, because phosphorylation generally regulates other receptor parameters. For example, phosphorylation of *N*-methyl-D-aspartate receptors modulates their affinity for agonist, desensitization, channel gating, and P_o but not channel conductance (23, 24). Protein kinase A phosphorylates GluR1 on Ser-845 and GluR6 on Ser-666 and Ser-684 and increases AMPA/kainate receptor responsiveness through modulation of channel gating and P_o but without reported changes in channel conductance (25–30). Interestingly, 5-HT_3 receptor channel conductance is potentiated similarly by protein kinase C through a redistribution of conductance states (31).

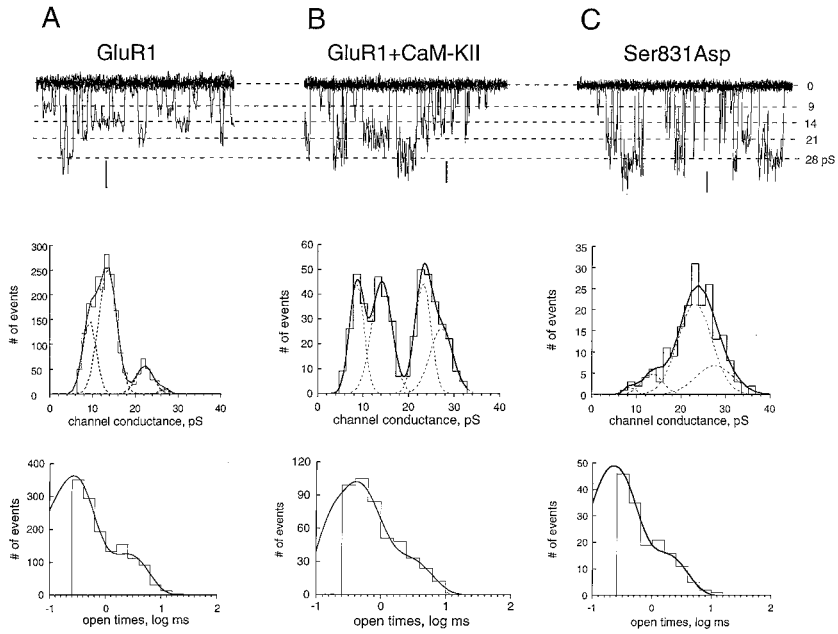

FIG. 4. CaM-KII increased the contribution of high-conductance states in single-channel activity. Single-channel recordings (*Top*), distribution of channel conductances (*Middle*), and channel openings (*Bottom*) were obtained from cells expressing GluR1 alone (*A*), from cells expressing GluR1 coexpressed with CaM-KII (*B*), or from the Ser-831-to-Asp mutant (*C*). For single-channel recordings, eight traces every 100 ms were superimposed, recorded at membrane potentials of −101 mV (A), −128 mV (*B*), and −125 mV (*C*). For comparison, currents in *A–C* were scaled by conductance and show the same four conductance states in all situations. Note the different scales for the same calibration of 1 pA in *A–C*. Each conductance histogram was fitted by the sum of four Gaussian functions (smooth curves), which are shown individually by dotted lines. Their mean values were, for *A*, 9.3 pS (contribution of 26.8%), 13.5 pS (56.8%), 22.2 pS (12.4%), and 27.3 pS (4%); for *B*, 8.6 pS (23.7%), 14.1 pS (30.3%), 23.1 pS (24%), and 27.1 (22%); and, for *C*, 9.6 pS (0.8%), 13.1 pS (13.7%), 21.3 pS (57.5%), and 26.1 pS (28%). Calculated weighted single-channel conductances were 13.8 pS (*A*), 17.9 pS (*B*), and 21.4 pS (*C*). Each distribution of open times was fitted by the sum of two exponentials with time constants of 0.24 ms (contribution of 73%) and 2.4 ms (*A*), 0.36 ms (71%) and 2.4 ms (*B*), and 0.29 ms (52%) and 2.5 ms (*C*).

During LTP, CA1 hippocampal AMPA-Rs are phosphorylated by CaM-KII on the GluR1 subunit (6); thus, one might expect that LTP would increase AMPA-R channel conductance. Because direct measurement of single-channel currents of postsynaptic AMPA-Rs in CA1 pyramidal neurons is not technically possible, Benke *et al.* (15) used nonstationary fluctuation analyses to show that induction of LTP often results in an increase (184 ± 20% of control) in single-channel conductance. Our single-channel observations not only provide direct support for the possibility of such regulation of postsynaptic AMPA receptor function, but they indicate the likely molecular mechanism for CaM-KII in the mediation of LTP as well. Particularly, phosphorylation by CaM-KII of the GluR1 subunit of AMPA-Rs increases the occurrence of higher conductance states, which enhances the total current through AMPA-Rs during their activation. CaM-KII uniquely phosphorylates GluR1 but not GluR2 (13, 14), suggesting an essential role of GluR1 in synaptic potentiation by CaM-KII. AMPA-Rs in the CA1 region of the hippocampus are comprised predominantly of GluR1 and GluR2 (32). GluR2 knockouts enhance LTP (33), and it becomes increasingly important to determine whether knockouts of GluR1 or homologous replacements of GluR1 with Ser-831-to-Ala mutants obviate expression of LTP in the CA1 region of the hippocampus, as suggested by an antisense approach (34).

An increase in AMPA-R channel conductance by CaM-KII phosphorylation may be, however, one of several mechanisms contributing to LTP. Indeed, the phenomenon of "silent" AMPA-R synapses that become functional on LTP induction can be explained better by an increase in the number of functional synaptic AMPA-Rs (35, 36). Infusion of activated CaM-KII into CA1 hippocampal neurons potentiates kainate-evoked currents in a manner consistent with the modulation of P_o or the number of channels (37). Furthermore, CaM-KII can increase exocytosis in dendrites of hippocampal neurons (38), and blocking membrane fusion in CA1 neurons reduces LTP (39). Although multiple mechanisms might contribute to LTP, our results, combined with the recent report by Benke *et al.* (15), indicate that one mechanism that enhances the responsiveness of postsynaptic AMPA-Rs during LTP is the CaM-

Table 2. CaM-KII (KII) increases contribution of high-conductance states in single-channel activity of GluR1

Receptor	γ_1, pS	γ_2, pS	γ_3, pS	γ_4, pS	$\gamma_3 + \gamma_4$,† %	γ,‡ pS	τ_{o1}, ms	τ_{o2}, ms	τ_{o1},§ %
R1	9.4 ± 0.3	13.6 ± 0.2	20.5 ± 0.8	28.3 ± 1.4	23 ± 2	12.6 ± 0.9	0.33 ± 0.07	2.1 ± 0.5	81 ± 4
	(6)	(6)	(6)	(6)	(6)	(6)	(6)	(6)	(6)
R1 + KII	7.6 ± 0.9	12.4 ± 0.6	19.3 ± 1.2	29.5 ± 2.0	55 ± 6**	18.2 ± 1.2**	0.43 ± 0.07	3.0 ± 0.7	70 ± 4
	(4)	(4)	(4)	(4)	(4)	(4)	(4)	(4)	(4)
S831D	8.4 ± 0.7	12.9 ± 1.0	22.2 ± 1.3	30.1 ± 1.8	83 ± 10**	21.5 ± 0.8**	0.41 ± 0.11	2.3 ± 0.7	71 ± 12
	(4)	(4)	(4)	(4)	(4)	(4)	(4)	(4)	(4)

Means + SEM are shown, with the number of measurements (in parentheses) below. **, $P < 0.01$.
†Combined contribution of γ_3 and γ_4 conductance states to the total distribution.
‡Weighted value (see *Experimental Methods*).
§Contribution of τ_{o1} to the total open times.

KII-mediated phosphorylation of AMPA-Rs, which increases channel conductance.

We thank Drs. Craig Jahr and Peter Jonas for critical reading of the manuscript. This work was supported by Jacob Javits Award NS27037 from the National Institutes of Health and by Human Frontier Science Program Organization Grant RG0030.

1. Bliss, T. V. P. & Collingridge, G. L. (1993) *Nature (London)* **361,** 31–39.
2. Nicoll, R. A. & Malenka, R. (1995) *Nature (London)* **377,** 115–118.
3. Fukunaga, K., Stoppini, L., Miyamoto, E. & Muller, D. (1993) *J. Biol. Chem.* **268,** 7863–7867.
4. Fukunaga, K., Muller, D. & Miyamoto, E. (1995) *J. Biol. Chem.* **270,** 6119–6124.
5. Giese, K. P., Fedorov, N. B., Filipkowski, R. K. & Silva, A. J. (1998) *Science* **279,** 870–873.
6. Barria, A., Muller, D., Derkach, V., Griffith, L. C. & Soderling, T. R. (1997) *Science* **276,** 2042–2045.
7. Miller, S. G. & Kennedy, M. B. (1986) *Cell* **44,** 861–870.
8. Lisman, J. (1994) *Trends Neurosci.* **17,** 406–408.
9. DeKoninck, P. & Schulman, H. (1998) *Science* **279,** 227–230.
10. McGlade-McCulloh, E., Yamamoto, H., Tan, S. E., Brickey, D. & Soderling, T. R. (1993) *Nature (London)* **362,** 640–642.
11. Pettit, D. L., Perlman, S. & Malinow, R. (1994) *Science* **266,** 1881–1885.
12. Lledo, P. M., Hjelmstad, G., Mukherji, S., Soderling, T. R., Malenka, R. & Nicoll, R. (1995) *Proc. Natl. Acad. Sci. USA* **92,** 11175–11179.
13. Barria, A., Derkach, V. & Soderling, T. R. (1997) *J. Biol. Chem.* **272,** 32727–32730.
14. Mammen, A. L., Kameyama, K., Roche, K. W. & Huganir, R. L. (1997) *J. Biol. Chem.* **272,** 32528–32533.
15. Benke, T. A., Luthi, A., Isaac, J. T. R. & Collingridge, G. L. (1998) *Nature (London)* **393,** 793–797.
16. Sigworth, F. J. (1980) *J. Physiol.* **307,** 97–129.
17. Colquhoun, D. & Sigworth, F. J. (1995) in *Single-Channel Recordings,* eds. Sakmann, B. & Neher, E. (Plenum, New York), pp. 483–587.
18. Bowie, D. & Mayer, M. L. (1995) *Neuron* **15,** 453–462.
19. Mosbacher, J., Schoepfer, R., Monyer, H., Burnashev, N., Seeburg, P. H. & Ruppersberg, J. P. (1994) *Science* **266,** 1059–1062.
20. Fleck, W., Bahring, R., Patneau, D. K. & Mayer, M. L. (1996) *J. Neurophysiol.* **75,** 2322–2333.
21. Hall, R. A. & Soderling, T. R. (1997) *Neurosci.* **78,** 361–371.
22. Swanson, G. T., Kamboj, S. K. & Cull-Candy, S. G. (1997) *J. Neurosci.* **17,** 58–69.
23. Lieberman, D. N. & Mody, I. (1994) *Nature (London)* **369,** 235–239.
24. Wang, L. Y., Orser, B. A., Brautigan, D. L. & MacDonald, J. F. (1994) *Nature (London)* **369,** 230–232.
25. Roche, K. W., O'Brien, R. J., Mammen, A. L., Bernhardt, J. & Huganir, R. L. (1996) *Neuron* **16,** 1179–1188.
26. Raymond, L. A., Blackstone, C. D. & Huganir, R. L. (1993) *Nature (London)* **361,** 637–641.
27. Wang, L. Y., Taverna, F. A., Huang, X. P., MacDonald, J. F. & Hampson, D. R. (1993) *Science* **259,** 1173–1175.
28. Wang, L. Y., Salter, M. W. & McDonald, J. F. (1991) *Science* **253,** 1132–1135.
29. Greengard, P., Jen, J., Nairn, A. C. & Stevens, C. F. (1991) *Science* **253,** 1135–1138.
30. Traynelis, S. F. & Wahl, P. (1997) *J. Physiol.* **503,** 513–531.
31. Van Hooft, J. A. & Vijverberg, H. P. (1995) *Recept. Channels* **3,** 7–12.
32. Petralia, R. & Wenthold, R. (1992) *J. Comp. Neurol.* **318,** 329–354.
33. Jia, Z., Agopyan, N., Miu, P. Z., Xiong, Z., Henderson, J., Gerlai, R., Taverna, F. A. A., Velumian, A., MacDonald, J., Carlen, P., *et al*. (1996) *Neuron* **17,** 945–956.
34. Vanderklish, P., Neve, R., Bahr, B. A., Arai, A., Hennegriff, M., Larson, J. & Lynch, G. (1992) *Synapse* **12,** 333–337.
35. Isaac, J. T., Nicoll, R. A. & Malenka, R. C. (1995) *Neuron* **15,** 427–434.
36. Liao, D., Hessler, N. A. & Malinow, R. (1995) *Nature (London)* **375,** 400–404.
37. Shirke, A. M. & Malinow, R. (1997) *J. Neurophysiol.* **78,** 2682–2692.
38. Maletic-Savatic, M. & Malinow, R. (1998) *J. Neurosci.* **18,** 6814–6821.
39. Lledo, P. M., Zhang, X., Sudhof, T. C., Malenka, R. C. & Nicoll, R. A. (1998) *Science* **279,** 399–403.